



HAL
open science

Cavity-Backed Broadband Microstrip Antenna Array for Photonic Beam Steering at W Band

Jérôme Taillieu, Ronan Sauleau, Mehdi Alouini, David Gonzalez-Ovejero

► **To cite this version:**

Jérôme Taillieu, Ronan Sauleau, Mehdi Alouini, David Gonzalez-Ovejero. Cavity-Backed Broadband Microstrip Antenna Array for Photonic Beam Steering at W Band. 16th European Conference on Antennas and Propagation (EuCAP 2022), Mar 2022, Madrid, Spain. 10.23919/EuCAP53622.2022.9769419 . hal-03771389

HAL Id: hal-03771389

<https://hal.science/hal-03771389v1>

Submitted on 26 Nov 2022

HAL is a multi-disciplinary open access archive for the deposit and dissemination of scientific research documents, whether they are published or not. The documents may come from teaching and research institutions in France or abroad, or from public or private research centers.

L'archive ouverte pluridisciplinaire **HAL**, est destinée au dépôt et à la diffusion de documents scientifiques de niveau recherche, publiés ou non, émanant des établissements d'enseignement et de recherche français ou étrangers, des laboratoires publics ou privés.

Cavity-Backed Broadband Microstrip Antenna Array for Photonic Beam Steering at W Band

Jérôme Taillieu^{1,2}, Ronan Sauleau¹, Mehdi Alouini², David González-Ovejero¹

¹ Univ Rennes, CNRS, IETR (Institut d'Électronique et des Technologies du numéRique) – UMR 61614, F-35000, Rennes, France, jerome.taillieu@univ-rennes1.fr *

² Univ Rennes, CNRS, Institut FOTON – UMR 6082, F-35000 Rennes, France

Abstract— We present here the design of a broadband antenna array for photonic beam-steering at W-band. The array unit-cell consists of two stacked microstrip patches that are cavity backed, and fed by aperture-coupling using an hourglass slot. The unit-cell shows a simulated impedance bandwidth of 37% for SWR<2 from 77 GHz to 112 GHz, thus covering most of the W band. The feeding network is designed using a low-loss Substrate Integrated Waveguide (SIW) and respects nearly the same bandwidth as the unit cell for a total SWR<2. Therefore, the structure is well-suited for fabrication by PCB technology. The final array is composed of 4 sub-arrays of 2×8 unit cells and exhibits a broadside directivity of 26 dBi. Each sub-array is expected to be fed by a Uni-Traveling-Carrier (UTC) photodiode, which enables power combining to overcome the low emitted power at mm-waves and also the use of optical phase shifters in the antenna architecture to achieve a +/-5° beam steering with reasonable grating lobes.

Index Terms—Beam steering, sub-mm waves, photonic carrier generation, cavity backed, stacked patch,

I. INTRODUCTION

Wireless data traffic increases by a factor of 100 every 10 years [1] and a more efficient use of the allocated spectrum will not suffice to reach the predicted data rates. The use of carriers in the millimeter (mm) or sub-mm wave regime will be pivotal to achieve the total bandwidths required for front- and back-hauling in beyond 5G systems, streaming of ultra-high definition multimedia and in data centers [2]-[3]. The development of continuous wave broadband sources with sufficient output power, such as UTC photodiodes, is one of the enabling technologies for future wireless systems [4]. These highly efficient components can pave the way for the photonic generation, modulation and treatment of mm- and sub-mm radio-frequency signals. Despite providing extremely wide bandwidths and presenting atmospheric transmission windows with attenuation levels below 10 dB/km, the use of sub-millimeter carriers is impaired by high propagation losses. To compensate these losses, one must use high power THz sources and high gain antennas

with beam steering capabilities to correct misalignment losses. Indeed, although fixed directive beams may suffice for short-range point-to-point (P2P) links, beam-steering is compulsory for P2P links for a fine self-alignment over longer distances.

Different solutions have been explored so far for photonic-enabled beam steering, such as tapered slot antennas (TSA) [5], horns [6], super-lattice photo-mixing arrays [7] or leaky-waves antennas [8]-[9]. These solutions are suitable for the photonic generation of the carrier, but are not easy to integrate into large 2D arrays because of the endfire radiation of TSAs, the large form factor of metallic horns and the inherent difficulty of integrating the photodiodes in arrays with a larger element count. Although leaky-wave antennas can exploit the wide frequency range provided by photonic generation, they suffer from a limited instantaneous bandwidth due to their frequency dispersion property. This work addresses the design of high-gain photonic-enabled phased array as a practical and low-cost solution for high-speed communications with the required 25dB of gain [10] for a reliable links, beam steering and taking advantage of power combining of high power THz sources.

This paper is organized as follows. Section II presents the emission chain for photonic beam steering. Section III deals with the unit-cell and sub-array design, performance and limitations. The beam steering capabilities and directivity of the total array are discussed in Section IV. Conclusions are drawn in Section V.

II. PHOTONIC-ENABLED BEAM STEERING

The overall antenna architecture relies on the photonic generation of the transmitted signal, thus benefiting from the relatively low-cost photonic components for amplification and high modulation speeds. Fig. 1 shows the intended scheme of the transmitter architecture. First, a dual frequency laser [11] at the optical C band is used to generate two highly correlated wavelengths $|\lambda_1 - \lambda_2| = 0.8\text{nm}$. Then, one of these optical carriers is modulated in phase and amplitude by a photonic IQ modulator in order to achieve a M-QAM modulation format. Then, this signal is amplified by an Erbium Doped Fiber Amplifier (EDFA) and filtered to

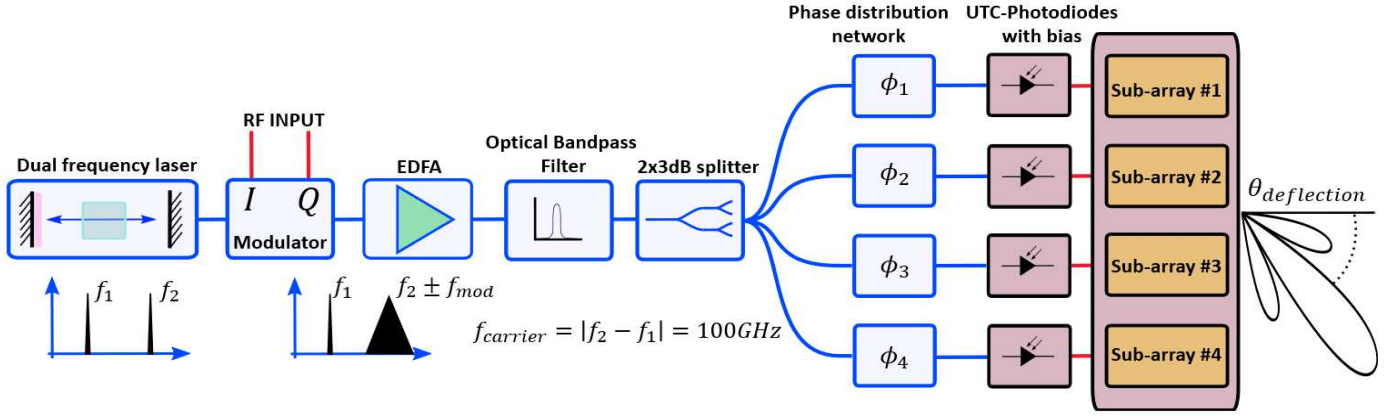


Fig. 1. Schematic of the emission chain

reduce the amplified spontaneous emission noise of the amplifier. Next, the amplification chain is split into four arms by a cascade of optical couplers. The phase shift distribution network will be assured, in the first instance, by a true time delay components [12] that precede the UTC photomixers and provide a quasi-infinite bandwidth without squint effect. The Phased Array Antenna (PAA) is composed of four subarrays, each excited by a single UTC-photodiode. The RF link will be established at the central frequency of 100 GHz in order to benefit from the mature technologies used in optical communications for optical wavelength, multiplexing and treatment.

III. ANTENNA GEOMETRY

A. The unit-cell

The proposed unit-cell is based on a multilayer PCB structure, thus combining the advantages of this low-cost PCB manufacturing process with a high integration level and a wide -3 dB gain bandwidth over most of the W band. In the mm- and sub-mm wave range, surface waves may severely impair the efficiency and scanning capabilities of antenna arrays. Therefore, an appropriate unit-cell must be found.

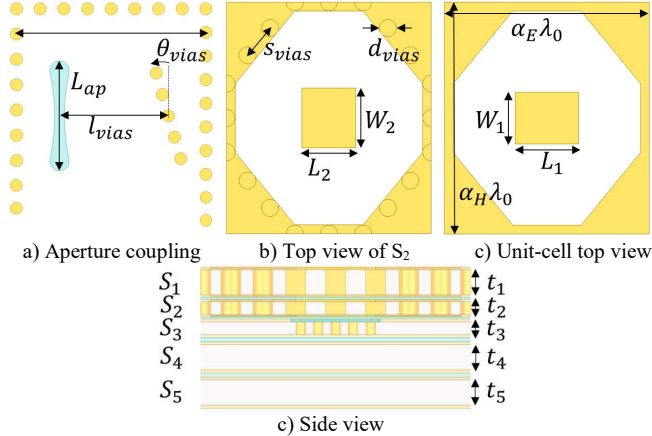


Fig. 2. Geometry and design variables for the array unit cell: (a) hourglass slot for aperture coupling, (b) Top view of the patch printed on S_2 , (c) Top view of the patch printed on S_1 , (c) Detail of the total stack-up, including substrates S_1 to S_3 , with the unit cell, and substrates S_4 and S_5 for the feeding network.

Fig. 2 shows the adopted unit-cell. It is composed of two dielectric layers of RT/Duroid™ 5880 ($\epsilon_r = 2.25$, $\tan\delta = 0.004$ at W band) with different standard thickness $t_1 = 254\mu\text{m}$ and $t_2 = 127\mu\text{m}$. All the dielectric layers of the array are bonded with the thermoplastic Rogers CuClad 6250 ($\epsilon_r = 2.37$, $\tan\delta = 0.006$ at W band).

The unit-cell has three resonances, two of them are obtained by the stacked patches, while the other one is due to the cavity. This configuration provides a wide simulated impedance bandwidth of 37% in an infinite array configuration in HFSS (see Fig. 4) [13]. The dimensions of the unit-cell are $0.8\lambda_0$ and $0.9\lambda_0$ in the E- and H- planes respectively. It is then guaranteed that only the fundamental TE_{11} mode is excited over the whole impedance bandwidth within the cavity formed by the vias round the patches.

The dimensions of the unit-cell directly impact the resonances of the cavity; therefore, a compromise between the impedance bandwidth and the size of the cavity in the E-plane has been found. To this end, the cell has been maintained as small as possible in this plane in order to assure relatively low side lobes and avoid the onset of grating lobes in the $\pm 10^\circ$ scanning range of interest in this plane. Furthermore, as the impedance bandwidth of the unit-cell is particularly wide, we must also evaluate the evolution of its directivity over the frequency band. The dimension of the unit-cell in its steering plane is then the largest size possible to assure a stable directivity of the array over all the frequency band in its sub-array configuration. The octagonal shape of the cavity has been chosen for design simplicity in order to approximate a circular cavity as it has been shown that circular ones exhibit slightly more directivity than rectangular cavities [14].

Table 1: Dimensions for the array unit-cell shown in Fig. 2 (in μm)

L_{ap}	S_{vias}	L_1	L_2
1000	400	740	630
L_{vias}	d_{vias}	W_1	W_2
950	200	600	700
θ_{vias}	t_1	t_2	t_3
23	254	127	127
	t_4	t_5	
	254	254	

B. The sub-array

Different wideband corporate feeding networks in PCB technologies has been proposed for high frequency antennas. Microstrip networks stand out by their simplicity and low manufacturing risks, but suffer from high losses (0.4dB/mm) and can excite surface waves, which can lead to scan blindness. The Grounded Co-Planar Waveguide (GCPW) presents lower losses (0.3dB/mm) and weaker excitation of surface waves. Although it could be a good candidate for the distribution network, it suffers from strict fabrication tolerances. Substrate Integrated Waveguides (SIWs) appear as a very convenient solution, since they solve all the issues listed above at the cost of a larger footprint, a dispersive mode and an important number of vias that slightly increase the manufacturing cost. In the case at hand, we have used a 127 μ m thick, which corresponds to substrate #3 in Fig. 2. In order to ensure low leakage of the SIW and a good metallization, the diameter Φ of the vias and the spacing s between vias are chosen to respect the ratios $\phi = t_i / 0.8$ and $s = 4\phi$, where t_i is the thickness of the i^{th} substrate. The effective width of the SIW has been set to 1.5 mm in order to be far enough from the cutoff frequency (67GHz) and to ensure that only the fundamental TE₁₀ mode is excited in the band of interest.

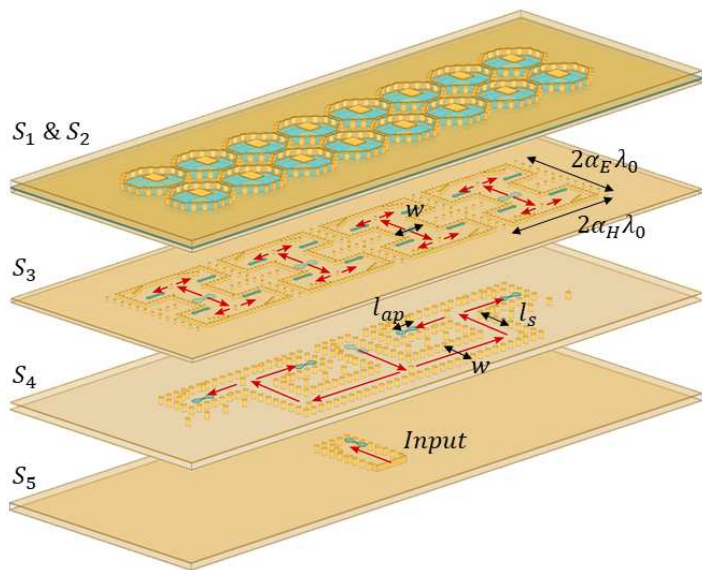


Fig. 3. 3D view of the sub-array stacked-up substrates and representation of the RF power path through the layers

Table 2: Main dimensions of the sub-array (μ m)

l_{ap}	w	l_s	λ_0
1000	1500	1590	3000
	α_E	α_H	
	0.8	0.9	

The sub-array, shown in Fig. 3, is composed of two elements in the steering plane (E-plane) and eight in the H-plane. Three substrates S_3 , S_4 and S_5 of RT/Duroid™ 5880 are stacked and coupled to each other through hourglass slots in order to maximize the impedance bandwidth. The input located at the substrate #5 is coupled to the substrate #4 using a coupling slot. The signal is then divided by a T-shape power divider followed by a right-angle bend. This bend is followed, less than a wavelength after, by another T-shape power divider. This distance (l_s in Fig. 3) is critical, such a short separation induces the excitation of reflected back higher order modes of the SIW. This distance could not be reduced for the imposed bandwidth.

Another sub-array configuration would have been possible by adding other layers of substrates in which the RF power would have been successively divided. However, this arrangement implies to multiply the number of substrate-to-substrate transitions with losses reach 0.6dB for 40 μ m thickness of pre-Preg. This would have reduced the number of elements and thus the directivity in favor of the deflection angle at the cost of higher losses. In the context where the number of photodiodes is limited due to manufacturing constraints and where the gain is the main figure of merit this option is not conceivable. The total width of the subarray in the steering plane has been set to two unit-cells. In order to maintain the distance of $0.8\lambda_0$ in the steering plane, the one-to-four sub-array in the substrate #3 has been designed to compensate the 90° phase shift in the hourglass slot at different sides of the cavity. The whole corporate feed network exhibits an SWR < 2 from 80GHz to 115GHz (see Fig. 4).

Each of the four sub-arrays will be fed by a UTC-photodiode [15] with an CPW output. The electrical connections with the PCB antenna will be assured by a silver epoxy glue to the GCPW at the back-side of substrate #5. It has to be taken into account for the total calculation of the losses that the UTC-photodiodes have a 50 Ω CPW output and do not compensate the high reactive part of the photodiode itself.

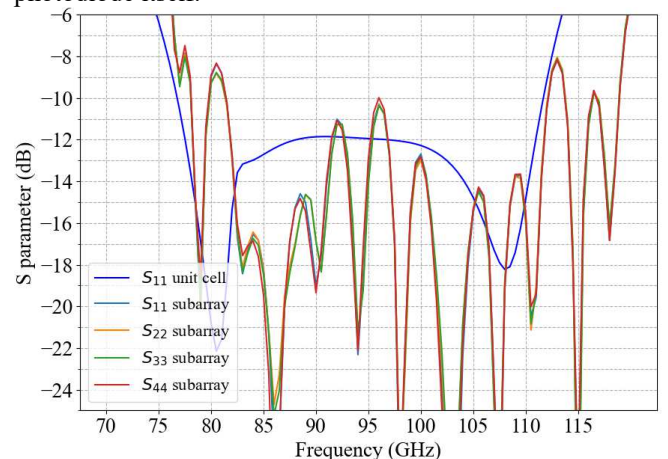


Fig. 4. Simulated reflection coefficients of the unit cell (with infinitely periodic array conditions) and the different subarrays

The complete array is composed of four subarrays each spaced of $2 \times 0.8\lambda_0$ in the steering plane which represent 19.2mm of width and 21.6mm of length. It has to be noted this subarray design allows to stack in the steering plane as many subarrays as wished, thus improving the directivity and taking the most of the power combining.

A lowpass RF choke has been designed for the bias of the photodiode, followed by a GCPW-to-SIW transition with a -20 dB input reflection coefficient over more than the W-band. For assembling convenience, the photodiodes are set by pair but are fed from independent fiber optics fixed to a V-Groove lensed fiber array with 500 μm separation. In practice, the coupling between the photodiode and the lensed fiber is the most critical part of the antenna regarding optical losses. A misalignment of 1.5 μm only induces 1.8 dB of optical losses which correspond to 2.6 dB of RF losses. To mitigate this effect by easing the assembly, the photodiodes are placed on opposite sides of the array and the fibers are glued using active feedback with a 6 axes nano-positioner stage. The electric and optical coupling is especially critical, in consequence we decided to limit the array to only four subarrays.

IV. RADIATION PATTERN

The total array is composed of four sub-arrays themselves counting 16 radiating elements which brings the total number of elements to 64. The simulated directivity of 26 dBi (Fig. 5) at 100 GHz broadside with 1.5 dB of total losses. The width of the sub-arrays ($1.6\lambda_0$) does not allow steering angles beyond $\pm 5^\circ$ but this dimension could not be substantially reduced. Nonetheless, an array with 26 dBi directivity is sufficient for medium-range links at W-band and the target scanning range, enough for an active compensation of the scanning.

Indeed, a single row (one element in the E-plane) sub-array would require two times more substrates layers for the feeding network, which would dramatically increase the manufacturing complexity and divide by two the number of radiating elements for the same number of photodiodes. In the presented configuration, the first side lobe is expected at -29° for a steering at $+5^\circ$ while assuring a stable 3dB gain bandwidth over the band of interest.

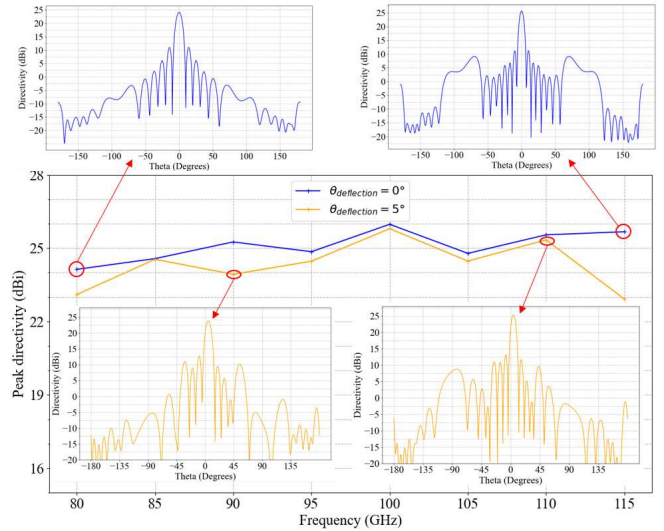


Fig. 5. Directivity of the total array at broadside (with its radiation patterns associated) and at 5 degrees according to the frequency

V. CONCLUSION AND PERSPECTIVES

A SIW fed array showing 26 dBi directivity over most of the W band has been presented. This array is compatible with low-cost PCB process, and it has been designed to be fed by four UTC-photodiodes taking thus advantage of photonic technologies for modulation and phase distribution network. It is composed of 64 radiating elements with a 37% relative impedance bandwidth compatible for integration into very large phased array. The limitations in gain and bandwidth are mainly due to the complexity of the optical and electrical coupling of the photodiodes which restrict their number. The realization of the 100GHz dual frequency laser is ongoing and will be ready as soon as the antenna will be manufactured.

ACKNOWLEDGMENT

The authors would like to thank the European Union financement through the European Regional Development Fund (ERDF), and the French region of Brittany, Ministry of Higher Education and Research, Rennes Métropole and Conseil Départemental 35, through the CPER Project SOPHIE / STIC & Ondes. This work has received a French government support granted to the Labex CominLabs excellence laboratory and managed by the National Research Agency in the “Investing for the Future” program under reference ANR-10-LABX-07-01.

REFERENCES

- [1] “Ericsson Mobility Report,” no. June, 2019.
- [2] T. Nagatsuma and G. Carpintero, “Recent progress and future prospect of photonics-enabled terahertz communications research,” *IEICE Trans. Electron.*, vol. E98C, no. 12, pp. 1060–1070, 2015
- [3] T. Nagatsuma, G. Ducourmau, and C. C. Renaud, “Advances in terahertz communications accelerated by photonics,” *Nat. Photonics*, vol. 10, no. 6, pp. 371–379, 2016
- [4] T. Nagatsuma, “Generating Millimeter and Terahertz Waves,” *IEEE Microw. Mag.*, vol. 10, no. 4, pp. 64–74, 2009

- [5] M. Ali, R. Cruzoe-Guzman, L. E. Garcia-Munoz, F. van Dijk, and G. Carpintero, "Photonics-enabled Millimetre-wave Phased-Array Antenna with True Time Delay Beam-steering," no. January, pp. 316–319, 2021
- [6] S. Rey, T. Merkle, A. Tessmann, and T. Kurner, "A phased array antenna with horn elements for 300 GHz communications," *ISAP 2016 - Int. Symp. Antennas Propag.*, pp. 122–123, 2017.
- [7] S. Preu *et al.*, "Fiber-Coupled 2-D n-i-pn-i-p Superlattice Photomixer Array," *IEEE Trans. Antennas Propag.*, vol. 65, no. 7, pp. 3474–3480, 2017
- [8] M. Steeg, P. Lu, J. Tebart, and A. Stohr, "2D mm-Wave Beam Steering via Optical True-Time Delay and Leaky-Wave Antennas," *GeMiC 2019 - 2019 Ger. Microw. Conf.*, pp. 158–161, 2019
- [9] Á. J. Pascual-Gracia *et al.*, "A photonically-excited leaky-wave antenna array at E-band for 1-D beam steering," *Appl. Sci.*, vol. 10, no. 10, pp. 1–16, 2020
- [10] A. J. Seeds, "Terahertz photonics for communications," *Opt. InfoBase Conf. Pap.*, vol. 33, no. 3, pp. 579–587, 2014
- [11] A. Rolland *et al.*, "Narrow Linewidth Tunable Terahertz Radiation By Photomixing Without Servo-Locking," pp. 260–266, 2014.
- [12] S. Pan, X. Ye, Y. Zhang, and F. Zhang, "Microwave Photonic Array Radars," *IEEE J. Microwaves*, vol. 1, no. 1, pp. 176–190, 2021
- [13] "ANSYS HFSS software, <http://www.ansoft.com/products/hf/hfss/>."
- [14] M. H. Awida and A. E. Fathy, "Design guidelines of substrate-integrated cavity-backed patch antennas," *IET Microwaves, Antennas Propag.*, vol. 6, no. 2, pp. 151–157, 2012
- [15] E. Rouvalis *et al.*, "High-speed photodiodes for InP-based photonic integrated," *2012 IEEE Photonics Conf. IPC 2012*, vol. 20, no. 8, pp. 88–89, 2012